# MAGNESIUM ALLOY AZ31B FORMING LIMIT CURVE USING THE NAKAZIMA TEST

**AUGUSTIN JITARU[1], COSMIN CONSTANTIN GRIGORAȘ[*1], GHEORGHE BRABIE[1], ANA-MARIA ROȘU[1], LUCIAN-MARIUS ROȘU[1]**

[1] *"Vasile Alecsandri" University of Bacau, Calea Mărăşeşti 157, Bacau, 600115, Romania*

**Abstract:** The behaviour of a metal sheet when forming can be predicted with accuracy if the forming limit curve is known (FLC). Generating an FLC is a two-step process that involves forming the material blanks and measuring the strain. This can be done by using the Marciniak or Nakazima tests. In this experimental paper, the Nakazima test was used and is conducted using a hemispherical punch, retaining plate, and draw beads, to prevent the blank from slipping, along with the ARAMIS digital image correlation (DIC) system, used for measuring. Metal sheets of magnesium alloy AZ31B were used, with thicknesses of 0.5 mm and 1.0 mm. The settings of the testing equipment have been selected to allow the material to break at different strains: from uniaxial to biaxial stretches. Each specimen represents specific stress in the strain limit diagram. The geometries of the material and its thicknesses have the same leading role in creating tensions. Compared to the tensile compression test, this test confirms better formability of sheets with a thickness of 0.5 mm.

**Keywords:** magnesium alloy, forming limit curve, Nakazima test, Aramis optical instruments

## 1. INTRODUCTION

Due to the increase in demand for lightweight materials for automobiles, aviation and electrical devices, magnesium alloys have attracted a lot of attention [1]. They are now used in various components such as laptops, computers, mobile phones, car structures. Conventionally, the above components in which magnesium alloys are used are made by pressure casting or injection. Press forming of magnesium alloys has recently attracted attention as it can extend the use of magnesium alloys [2]. However, there are very few applications of press forming, as magnesium alloys have low deformation at room temperature, mainly due to the limited number of sliding systems in the compact hexagonal network of magnesium alloys. Due to the critical shearing of non-basal sliding systems that decrease appreciably with the increase of deformation temperatures, hot deformation is one of the most effective plastic deformation methods of magnesium alloys [3]. Recently, hot deformation has aroused much interest, and numerous studies have been conducted mainly on the process of deep drawing. Crack failure in sheet forming is a significant concern when deforming processes are applied for thick metal plates [1]. Material thinning leads to plastic instability and represents a significant concern when dealing with magnesium-based alloys [1, 2]. Formability tests have to be conducted to understand the material behaviour better and generate forming limit diagrams (FLD). These tests range from physical (Nakazima formability test) [4] to numerical using the classical finite element method (FEM) [5] or crystal plasticity finite element (CPFE) [6]. High interest in magnesium alloys can be observed through the science community [1-6]. AZ31, AZ61, AZ91, ZE10, ZEK100, WE43, Mg–7Li–1Zn or AZMX3110 magnesium alloys are tested in various conditions so that

[*] Corresponding author, email: cosmin.grigoras@ub.ro
doi.org/10.29081/jesr.v28i1.006

the formability limits can increase; such processes include the variation of temperature from room temperature to above 300°C [3] or by grain refinement [7].

Automatic strain measurement systems are used to determine the formability limits; solutions such as ASAME, or GOM ARAMIS are the preferred choices. [4, 8].

The formability of an alloy is its ability to pass through plastic deformation without being damaged or broken [9-12]. The deformation characteristics of magnesium alloys are not so often analyzed, and most researchers have limited their studies to AZ31 [2, 3, 5, 7, 12], which is the most common/standard commercial magnesium alloy. Most of the research is related to uniaxial traction tests at different temperatures, based on which many authors have made predictions.

Drawing is the technological operation in which a semi-manufactured flat metal sheet is transformed, by plastic deformation, into a finite part, as shown in Figure 1. The operation can also further modify the part to increase its depth. A vast range of parts is executed by drawing, different in both shape and size. This process is widely used in the automotive industry, the aviation industry, the food industry, as well as other industrial fields [13-15], due to the following advantages: reduced material consumption, simple processing operations, high processing accuracy, the low-cost price versus cutting, the possibility of obtaining complex forms with a minimum number of operations and reduced labour, the possibility of automation (automation lines and flexible manufacturing cells), fast execution cycle, use in cases where the geometry of the product is difficult to obtain by other manufacturing processes, the possibility of obtaining parts with significant strength for minimum weight.

The disadvantages of the drawing process are high initial investments in tool execution, high maintenance cost, and high forces for deformation.

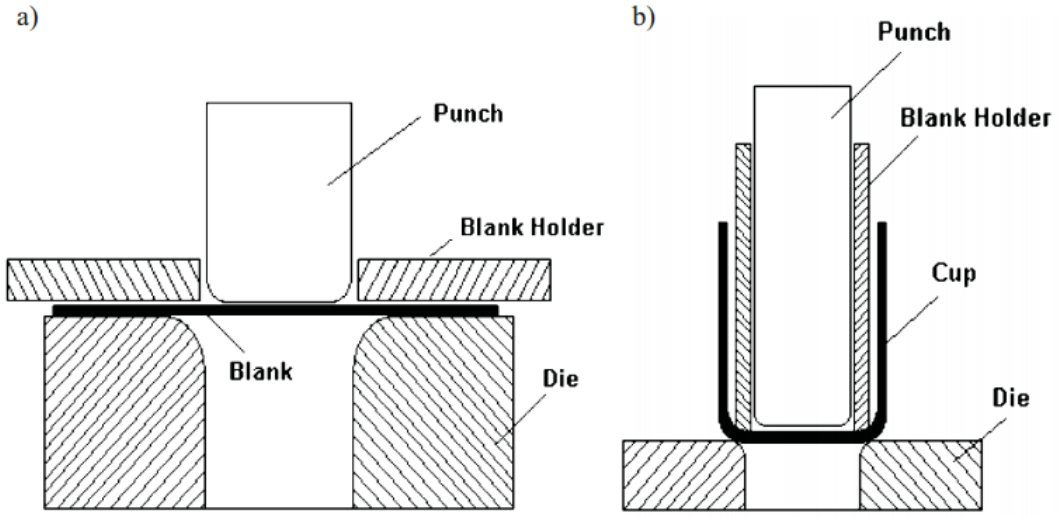


Fig. 1. Drawing schematic representation process.

## 2. EXPERIMENTAL SETUP

The most well-known formability tests for magnesium alloys are Nakazima and Marciniak [16, 17]. The most crucial difference between these tests is the shape of the spherical punch and the retaining method. For this experimental paper, the Nakazima test was chosen to be the simplicity of the process. A mold, a semispherical punch, a retaining plate, and draw beads are used for the Nakazima test to prevent the blank from slipping. The experiment was conducted on AZ31B magnesium alloy sheets of 1 mm and 0.5 mm in thickness. The process parameters have been selected to allow the material to break at different strains: from uniaxial to biaxial stretches. Different dimensions are required for these tests to generate different stages of deformation. Each test part represents specific strain in the forming limit diagram. The Aramis optical measuring instruments, shown in Figure 2, was used to measure the strain deformation limits (FDL).

The deformation of the geometries used the optimal parameters for the experiment process are deformation speed of 50 mm/min, deformation force of 50 kN, and 60 mm punch stroke. For the test to be conducted, a layer of paint was sprayed over the samples so that the Aramis system could track individual points. Figure 3 shows the shape and dimensions of the test blanks used along with the deformed shapes obtained after the Nakazima test. The samples show the phenomenon of necking and breaking at the end of the test.

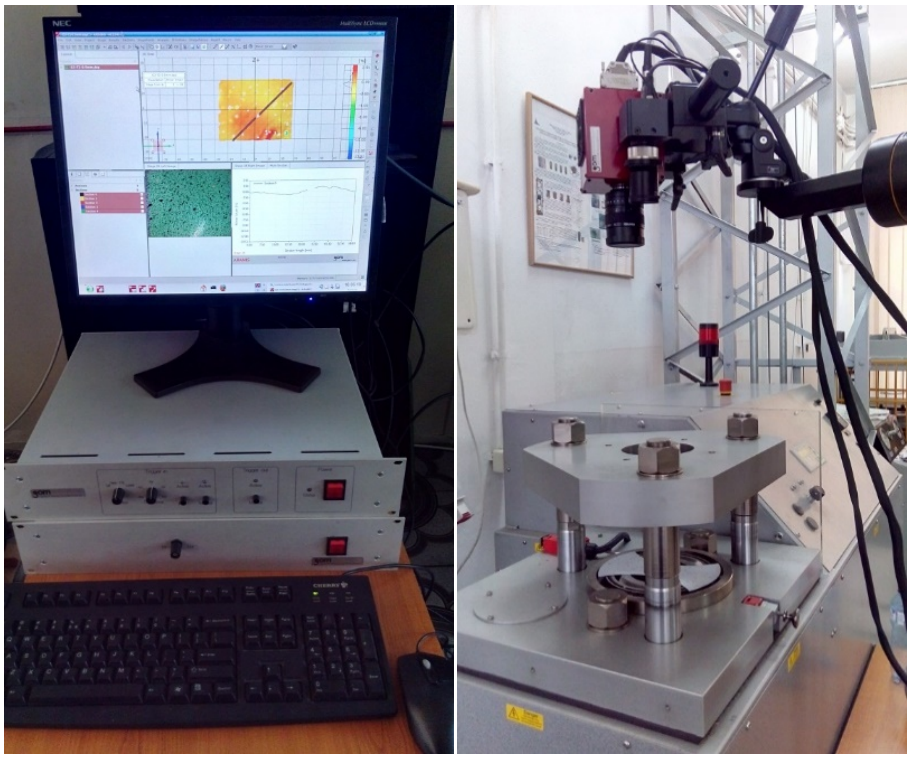

Fig. 2. Nakazima test setup highlighting the software and hardware components of the GOM Aramis system along with the hydraulic press.

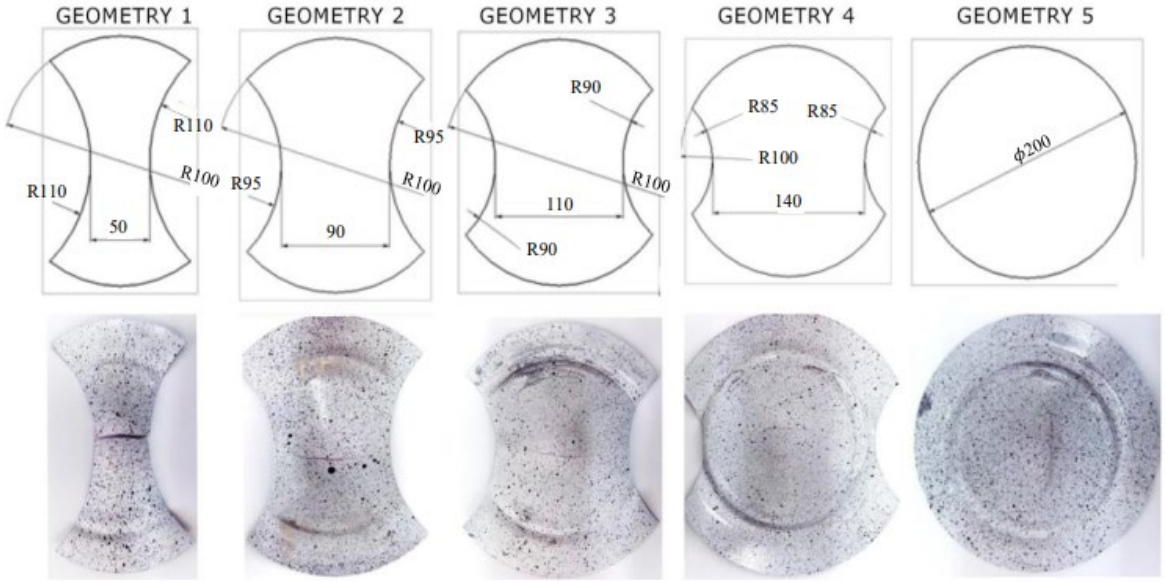


Fig. 3. Blanks geometries before and after the Nakazima test.

The chemical composition, as indicated by the manufacturer (CNMAGALLOY) is presented in Table 1. The mechanical properties, highlighted in Table 2, of the magnesium alloy AZ31B used in this experimental study,

are from both the manufacturer and where also determined on a material tensile test machine (Lloyd EZ50), using an Epsilon-3532 extensometer.

Table 1. AZ31B magnesium alloy chemical composition.

| Al [%] | Ca [%] | Cu [%] | Fe [%] | Mg [%] | Mn [%] | Ni [%] | Si [%] | Zn [%] |
|---|---|---|---|---|---|---|---|---|
| 2.5-3.5 | < 0.04 | < 0.05 | < 0.005 | 97 | > 0.2 | < 0.005 | < 0.1 | 0.6 – 1.4 |

Table 2. AZ31B magnesium alloy mechanical properties.

| Yield strength $R_{p0,2}$ [MPa] | Tensile strength Rm [MPa] | Elongation for max. Load $A_{gt}$ [%] | Plastic strain ratio r | Poisson's ratio ν | Young modulus E [MPa] |
|---|---|---|---|---|---|
| 150 | 255 | 21 | 1.231 | 0.35 | 45000 |

## 3. RESULTS AND DISCUSSION

The test results are displayed as graphs for each material thickness, indicating the minimum and maximum strain for each analyzed geometry. As shown in Figure 4, the minimum and maximum strain values for the 0.5 mm thickness material are similar and are reaching from 0.03 to 0.04. Geometries 3 through 5 behaviour is different when comparing the strain evolution as the punch stroke increases. As the maximum strain increases to values ranging from 0.05 to 0.08, the minimum values remain under 0.01. Another aspect that emerged is that the material shaped as Geometry 5 presented failure at a 40 mm stroke, compared to 60 mm that corresponds to Geometry 3. The most prominent strain is located at a 30 mm stroke for Geometries 1 through 3, while Geometries 4 and 5 developed at an above 40 mm stroke.

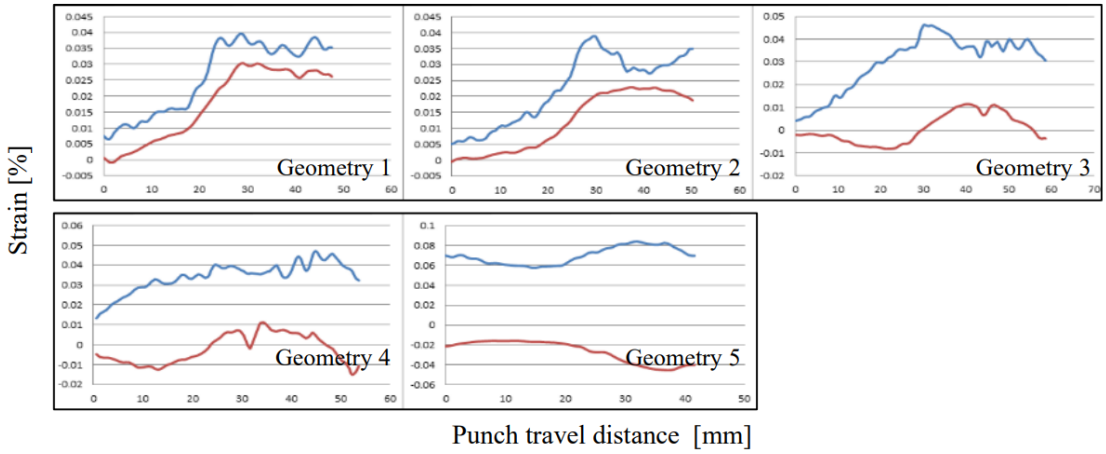


Fig. 4. Deformation values were obtained for the 0.5 mm thickness sheets as the minor (red line) and major (blue line) strain for geometry 1 to 5; punch travel distance on X-axes, by strain values on Y-axes.

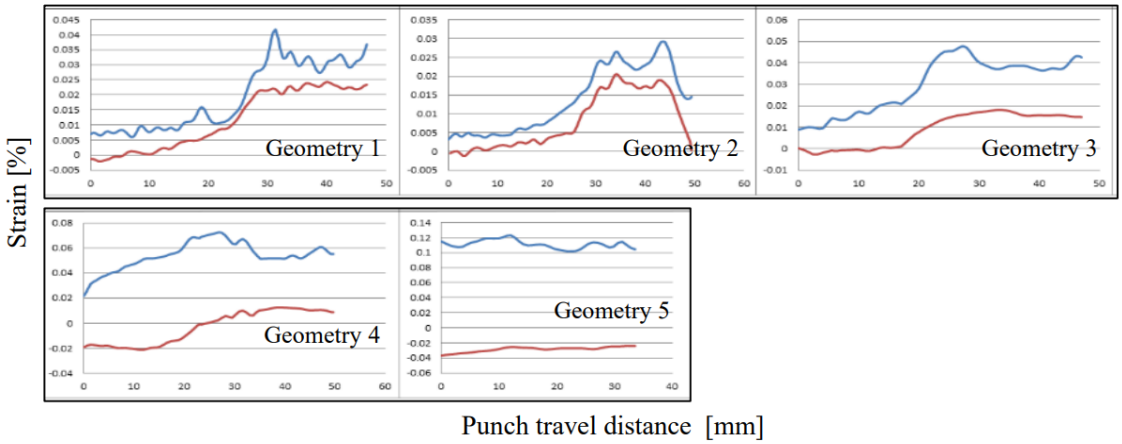


Fig. 5. Deformation values were obtained for the 1 mm thickness sheets as the minor (red line) and major (blue line) strain for geometry 1 to 5; punch travel distance on X-axes, by strain values on Y-axes.

Similar behaviour can be observed for the 1 mm thickness sheets. Figure 5 indicates that failure occurs in the region of 50 mm stroker. Higher values of the major strain were observed for Geometries 2 to 5 as values range from 0.05 to 0.12.

The strain increases can be seen in both 0,5 mm and 1mm thick boards. Compared to a 1 mm-thick plate, the 0.5 mm thick ones support lower stran and, at the same time, a more extended elongation with a longer breaking time.

The forming limit diagram is composed of interpreting the data obtained. These values, indicated in Table 3, were used to plot the forming limit curves (FLC) from Figure 6. Each of these curves indicates, for each thickness, two areas that represent the safe region for deformation (below the FLC) and the failure region (above FLC), while negative minor strain values indicate tension-compression drawing and positive ones indicate biaxial deformation. Thus, by comparing the two deformation curves, it can be noted observed that the 0.5 mm thickness sheets present higher formability.

Table 3. AZ31B magnesium alloy FLD values for minor and major strain, for both material thickness

| Geometry | 0.5 mm thickness | | 1 mm thickness | |
|---|---|---|---|---|
| | Minor strain % | Major strain % | Minor strain % | Major strain % |
| 5 | -0.0256 | 0.1223 | -0.0378 | 0.0824 |
| 4 | -0.0025 | 0.0357 | -0.0079 | 0.0331 |
| 3 | 0.0055 | 0.0422 | -0.0003 | 0.0044 |
| 2 | 0.0189 | 0.0596 | 0.0172 | 0.0364 |
| 1 | 0.0233 | 0.0665 | 0.0287 | 0.0383 |

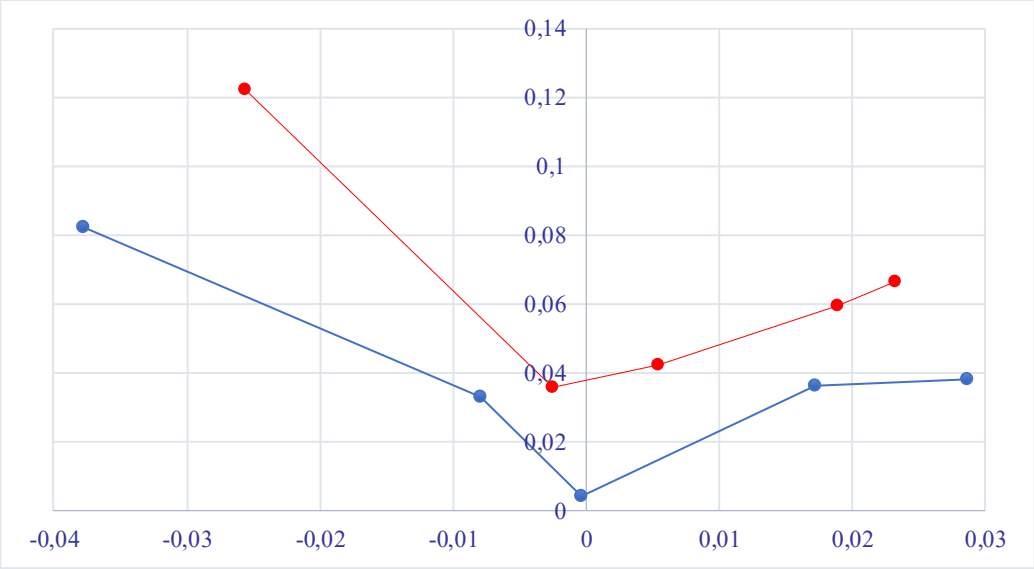


Fig. 6. Forming limit curve (FLC) obtained for the magnesium alloy AZ31B using the Nakazima test for the 0.5 mm (red line) and 1 mm (blue line) thicknesses; minor string on X-axes by major strain on the Y-axes.

## 4. CONCLUSIONS

The Nakazima test was conducted to investigate the forming limit curve for the magnesium alloy AZ31B, for both 0.5 and 1.0 mm thicknesses. The FLC were obtained through the GOM Aramis image overlay system. The primary role in creating tensions is the geometry of the material as well as its thicknesses. Compared to a compression-stretching test, these results confirms better formability of the boards with thicknesses of 0,5 mm.
The variation in thickness plays an essential role in the deformation capacity of magnesium alloys; it was shown that thinner sheets can be plastically deformed with ease, as espected. Furthemore, the values highlited in the FLD indicate that this alloy is hard to deforme at room temperature. By comparing the data to other alloys such

as steel or aluminium based ones, it can be noted that the plasticity of the AZ31B is much lower; this is translated in premature failure, with cracks appering and propagating suddenly with not or very little observation of plastic deformation.

**REFERENCES**

[1] Kumar, S.D., Amjith, T.R., Anjaneyulu, C., Forming limit diagram generation of aluminum alloy AA2014 using nakazima test simulation tool, Procedia Technology, vol. 24, 2016, p. 386-393.
[2] Xue, F., Yan, Y., Kang, J., Predicting forming limit diagrams for AZ31 magnesium alloy and 7050 aluminum alloy by numerical simulation, The Journal of Strain Analysis for Engineering Design, vol. 56, no. 8, 2020, p. 598-608.
[3] Boba, M., Butcher, C., Panahi, N., Worswick, M.J., Mishra, R.K., Carter, J.T., Warm forming limits of rare earth-magnesium alloy ZEK100 sheet, International Journal of Material Forming, vol. 10, no. 2, 2017, p. 181-191.
[4] Lumelskyj, D., Rojek, J., Banabic, D., Lazarescu, L., Detection of strain localization in nakazima formability test - experimental research and numerical simulation, Procedia Engineering, vol. 183, 2017, p. 89-94.
[5] Mekonen, M.N., Steglich, D., Bohlen, J., Letzig, D., Mosler, J., Experimental and numerical investigation of Mg alloy sheet formability, Materials Science and Engineering, vol. 586, 2013, p. 204-214.
[6] Bong, H.J., Lee, J., Hu, X., Sun, X., Lee, M.G., Predicting forming limit diagrams for magnesium alloys using crystal plasticity finite elements, International Journal of Plasticity, vol. 126, 2020, p. 102630.
[7] Somekawa, H., Nakajima, K., Singh, A., Mukai, T., Ductile fracture mechanism in fine-grained magnesium alloy, Philosophical Magazine Letters, vol. 90, no. 11, 2010, p. 831-839.
[8] Ayachi, N., Guermazi, N., Pham, C.H., Manach, P.Y., Development of a nakazima test suitable for determining the formability of ultra-thin copper sheets, Metals, vol. 10, no. 9, 2020 p. 1163.
[9] Bloeck, M., Advanced materials in automotive engineering, Ed. Woodhead Publishing, 2012
[10] Chino, Y., Enhanced room temperature formability of magnesium alloy sheets by suppression of basal texture formation, Journal of Physics, Conference Series, 1063, 2018, p. 012008.
[11] Yang, Q., Jiang, B., Wang, L., Dai, J., Zhang, J., Pan, F., Enhanced formability of a magnesium alloy sheet via in-plane pre-strain paths, Journal of Alloys and Compounds, vol. 814, 2020, p. 152278.
[12] Zhang, H., Huang, G.S., Song, B., Zhang, L., Kong, D.Q., Influence of microstructure and texture on formability of AZ31B magnesium alloy sheets, Transactions of Nonferrous Metals Society of China, vol. 21, no. 4, 2011, p. 844-850.
[13] Dwivedi, R., Agnihotri, G., Study of deep drawing process parameters, Materials Today: Proceedings,. vol. 4, no. 2, 2017, p. 820-826.
[14] The-Thanh, L., Tien-Long, B., The-Van, T., A study on a deep-drawing process with two shaping states for a fuel-filter cup using combined simulation and experiment, Advances in Mechanical Engineering, vol. 11, no. 8, 2019, p. 1-11.
[15] Zaid, A.I.O., Deep drawing mechanism, parameters, defects and recent results: state of the art, IOP Conference Series: Materials Science and Engineering, vol. 146, 2016, p. 012009.
[16] Gutiérrez, D., Lara, A., Casellas, D., Prado, J.M., Effect of strain paths on formability evaluation of TRIP steels, Advanced Materials Research, vol. 89-91, 2010, p. 214-219.
[17] Noder, J., Butcher, C., A comparative investigation into the influence of the constitutive model on the prediction of in-plane formability for Nakazima and Marciniak tests, International Journal of Mechanical Sciences, vol. 163, 2019, p. 105138.